WWW.IJRPR.COM

International Journal of Research Publication and Reviews

Journal homepage: www.ijrpr.com ISSN 2582-7421

Evaluation of a Polyherbal Formulation from Acorus calamus, Glycyrrhiza glabra, Symplocos racemosa, and Coriandrum sativum for Anti-Acne Efficacy and Safety

Km.Kavita[1]*, Shaily Mishra[1], Dr. Shamim Ahmad[1]

[1]Translam Institute of Pharmaceutical Education and Research, Meerut Uttar pradesh
Corresponding author: Km.Kavita1
Email ID -kavitavrtma@gmail.com
Associate Professor, Translam Institute of Pharmaceutical Education and Research, Meerut Uttar pradesh

ABSTRACT :

Acne vulgaris, a prevalent chronic inflammatory skin condition, poses significant physical and psychological challenges globally. This study investigates the anti-acne efficacy of a polyherbal formulation comprising extracts from *Acorus calamus*, *Glycyrrhiza glabra*, *Symplocos racemosa*, and *Coriandrum sativum*. Sequential Soxhlet extraction using petroleum ether, ethyl acetate, and methanol yielded crude extracts, with methanol extracts showing the highest yields (9.2–12.0% w/w) and diverse phytochemical profiles, including alkaloids, flavonoids, and terpenoids. Four bioactive compounds—β-asarone, glycyrrhizin, quercetin, and linalool—were isolated and characterized via NMR and mass spectrometry. The polyherbal formulation demonstrated superior in vitro antibacterial activity against *Propionibacterium acnes* and *Staphylococcus epidermidis* (MIC: 5.5 and 7.0 µg/mL, respectively), sebum reduction (47.2 ± 2.4%), and nitric oxide inhibition (40.5 ± 2.2%) compared to individual extracts and compounds. Synergistic effects were confirmed with FIC indices of 0.30 ± 0.03 (*P. acnes*) and 0.38 ± 0.04 (*S. epidermidis*). In vivo studies in Wistar rats showed a 68.4 ± 3.5% reduction in acne lesions after 14 days. The formulation exhibited no skin irritation, high cell viability (94.5 ± 1.9%), and stability under accelerated conditions for 6 months. These findings suggest the polyherbal formulation as a promising, safe, and effective alternative for acne management, warranting further clinical evaluation.

Keywords :- β-asarone, Acorus calamus, Glycyrrhiza glabra, Symplocos racemosa, and Coriandrum sativum.

Introduction

Acne vulgaris is a chronic inflammatory dermatological condition characterized by the formation of comedones, papules, pustules, nodules, and cysts, primarily affecting the pilosebaceous units of the skin. It manifests predominantly on the face, chest, and back, areas rich in sebaceous glands. The condition results from a complex interplay of factors, including excessive sebum production, follicular hyperkeratinization, colonization by *Cutibacterium acnes* (formerly *Propionibacterium acnes*), and inflammatory responses [1]. Acne vulgaris is not merely a cosmetic concern; it significantly impacts physical, psychological, and social well-being, often leading to scarring, hyperpigmentation, and diminished quality of life [2]. This introduction provides an overview of acne vulgaris, its global prevalence, and the critical need for innovative therapeutic approaches, supported by contemporary research. Acne vulgaris is a multifactorial disease influenced by genetic, hormonal, environmental, and microbial factors. The condition typically emerges during puberty due to increased androgen levels, which stimulate sebaceous gland activity and sebum production [3]. Sebum, an oily substance, combines with dead skin cells to obstruct hair follicles, creating an environment conducive to the proliferation of *C. acnes*. This triggers an immune response, leading to inflammation and lesion formation [4]. The clinical presentation varies from mild comedonal acne to severe cystic forms, with severity influenced by factors such as stress, diet, and skincare practices [5]. Beyond physical symptoms, acne vulgaris is associated with psychological distress, including anxiety, social withdrawal, and depression, particularly in adolescents and young adults [6]. The chronic nature of acne, coupled with its potential for permanent scarring, underscores the importance of early and effective management [7].Acne vulgaris is one of the most common skin disorders worldwide, affecting individuals across age groups, ethnicities, and genders. Epidemiological studies estimate that approximately 9.4% of the global population, or over 700 million people, are affected by acne at any given time [8]. The prevalence is highest among adolescents, with up to 85% of individuals aged 12–24 years experiencing some form of acne [9]. While acne is often associated with puberty, it persists into adulthood in a significant proportion of cases, particularly among women, with studies reporting a prevalence of 20–40% in adults over 25 years [10]. Regional variations exist, with higher rates observed in urbanized areas and populations with Westernized diets high in dairy and refined carbohydrates [11]. Acne also disproportionately affects certain ethnic groups, with individuals of African descent more prone to post-inflammatory hyperpigmentation and scarring [12]. The widespread prevalence of acne vulgaris highlights its status as a global public health concern, necessitating accessible and effective treatment options [13]. Despite the availability of numerous treatments, including topical retinoids, benzoyl peroxide, antibiotics, and systemic isotretinoin, significant challenges persist in the management of acne vulgaris. Current therapies often yield suboptimal outcomes due to variable efficacy, side effects,

and poor patient adherence [14]. For instance, prolonged use of topical and oral antibiotics has contributed to the emergence of antibiotic-resistant strains of *C. acnes*, reducing treatment efficacy and posing a public health threat [15]. Systemic isotretinoin, while highly effective for severe acne, is associated with significant adverse effects, including teratogenicity, hepatotoxicity, and psychiatric symptoms, limiting its use in certain populations [16]. Moreover, many patients experience relapse after treatment cessation, with studies reporting recurrence rates of 20–40% within one year [17]. The psychological burden of acne further complicates treatment, as patients with persistent or treatment-resistant acne often report diminished self-esteem and increased mental health challenges [18].

The limitations of existing therapies underscore the urgent need for novel treatment modalities that address the multifactorial pathogenesis of acne vulgaris. Recent advances in dermatological research have explored targeted therapies, such as sebum-regulating agents, anti-inflammatory biologics, and microbiome-modulating treatments [19]. For example, inhibitors of acetyl-CoA carboxylase, an enzyme involved in sebum synthesis, have shown promise in reducing sebum production and lesion counts in early clinical trials [20]. Similarly, probiotic and bacteriophage therapies aimed at modulating the skin microbiome offer potential alternatives to antibiotics [21]. Additionally, there is growing interest in personalized medicine approaches, leveraging genetic and biomarker data to tailor treatments to individual patient profiles [22]. These emerging strategies hold promise for improving therapeutic outcomes and reducing the physical and psychological burden of acne vulgaris.

In conclusion, acne vulgaris remains a prevalent and complex dermatological condition with significant physical, emotional, and social implications. Its global burden, coupled with the limitations of current treatments, necessitates continued research into innovative and effective therapies. This study aims to contribute to this effort by investigating novel approaches to acne management, addressing unmet needs in treatment efficacy, safety, and patient satisfaction.

Materials Required

Plant Materials

Fresh Acorus calamus (rhizomes), Glycyrrhiza glabra (roots), Symplocos racemosa (bark), and Coriandrum sativum (seeds) (2.5 kg each) were sourced from Himalaya Herbal Supplies, Dehradun, India. Authenticated by the Botanical Survey of India (Voucher Nos. BSI/NRC/2024/001–004), materials were air-dried at 40°C, ground into powder using a Pulverizer 2HP (Bharat Machinery), and stored at room temperature.

Solvents and Chemicals

Analytical-grade solvents from Merck India included hexane (6 L), ethyl acetate (10 L), methanol (15 L), and petroleum ether (12 L, 60–80°C). Sigma-Aldrich supplied deuterated chloroform-d and methanol-d4 (10 mL each) for NMR. Phytochemical reagents (Salkowski's, Shinoda's, Dragendorff's, ferric chloride) and MS-grade acetonitrile, formic acid, iodine crystals, and anhydrous sodium sulfate were procured from approved vendors meeting Indian Pharmacopoeia standards.

Extraction and Isolation Equipment

Soxhlet extractors (Borosil, 500 mL) processed 100 g plant material with 300 mL solvent per cycle. Extracts were concentrated using a Heidolph Laborota 4000 rotary evaporator at 40°C under vacuum. Silica gel (60–120 mesh, Merck) in 50 cm × 3 cm glass columns served as the stationary phase. Precoated TLC plates (Merck Silica Gel 60 F254) were visualized with iodine vapor and UV (254/366 nm). Whatman No. 1 filter paper and a vacuum filtration unit aided filtration.

Analytical Instruments

A Shimadzu UV-1800 spectrophotometer measured absorbance (200–800 nm). A 400 MHz Bruker Avance III NMR spectrometer analyzed compounds in 5 mm NMR tubes with deuterated solvents. An Agilent 6545 Q-TOF LC/MS with ESI determined molecular weights. Additional equipment included a Mettler Toledo balance (0.1 mg sensitivity), Elico LI 120 pH meter, Remi C-24 Plus centrifuge, LG refrigerator (4°C), Equitron water bath, and Labline hot air oven (250°C).

Microbiological and Cell Culture Materials

Staphylococcus epidermidis (ATCC 12228) and Propionibacterium acnes (ATCC 6919) cultures from MTCC, Chandigarh, were grown in nutrient agar/brain-heart infusion broth with anaerobic gas packs (HiMedia) for P. acnes. MIC and disc diffusion tests used 96-well plates (Tarsons) and 6 mm filter discs (HiMedia). Seb-1 human sebocytes were cultured in DMEM with 10% FBS and penicillin-streptomycin in a Thermo Scientific CO2 incubator, observed via an Olympus CKX41 microscope.

Formulation and Safety Testing Materials

Polyherbal gels used carbopol 940, propylene glycol, cetyl alcohol, and triethanolamine (Loba Chemie). Safety tests on 24 Wistar rats (150–200 g, IAEC/2024/03) involved 3M Tegaderm patch tests, digital Vernier caliper for skin thickness, and hematoxylin-eosin staining for histopathology.

Documentation and Consumables

Data were recorded in lab notebooks, digitized in Microsoft Excel, and analyzed with SPSS (v26) and GraphPad Prism (v9). Reports were prepared using Microsoft Office and Adobe Acrobat Pro. NMR and MS data were processed with Bruker TopSpin and Agilent MassHunter. Consumables included micropipette tips, syringes, sterile glassware, PPE, Milli-Q water, and MS/NMR-compatible vials/tubes.

Methodology

Collection and Authentication

Plant materials (2.5 kg each) from Himalaya Herbal Supplies were authenticated (BSI/NRC/2024/001–004), air-dried at 40°C for 48 hours, ground, and stored.

Extract Preparation

Sequential Soxhlet extraction (8 hours, 100 g material, 300 mL solvent: methanol, petroleum ether, ethyl acetate) yielded crude extracts, filtered (Whatman No. 1), concentrated at 40°C, weighed, and stored at 4°C.

Bioactive Compound Isolation

Crude extracts (2 g) were separated via column chromatography (silica gel, 60–120 mesh) using hexane, hexane:ethyl acetate gradients, and methanol. TLC (Merck Silica Gel 60 F254) monitored fractions (10 mL), visualized with iodine/UV. Similar fractions were pooled, concentrated, and stored at 4°C.

Compound Characterization

Isolated compounds (10 mg) were analyzed by 400 MHz NMR (Bruker Avance III) in chloroform-d/methanol-d4. MS (Agilent 6545 Q-TOF, ESI) used acetonitrile with 0.1% formic acid. UV-visible spectroscopy (Shimadzu UV-1800) assessed absorbance (200–800 nm).

Phytochemical Analysis

Crude extracts and compounds were screened for terpenoids (Salkowski's), flavonoids (Shinoda's), tannins (ferric chloride), and alkaloids (Dragendorff's) using standard tests.

Polyherbal Formulation

Extracts or compounds (1:1:1:1 w/w) were mixed with carbopol 940 (1%), propylene glycol (5%), cetyl alcohol (2%), and triethanolamine to form a gel, homogenized, and stored at 4°C.

In Vitro Anti-Acne Evaluation

Antibacterial activity against P. acnes and S. epidermidis was tested via disc diffusion (10 µL, 10 mg/mL) and MIC (0.1–100 µg/mL) assays. Sebum reduction was assessed in Seb-1 cells (10–100 µg/mL) using a lipid assay kit after 48 hours.

Synergy and Comparative Analysis

Synergistic effects were evaluated using the checkerboard assay (FIC ≤0.5). Solvent extracts were compared for efficacy. Statistical analysis used SPSS (v26) with ANOVA and Tukey's test ($p < 0.05$).

Safety Assessment

Polyherbal gel (0.5 g/cm2) was applied to Wistar rats (n=24, IAEC/2024/03). Skin irritation was scored per OECD guidelines after 24/48 hours. Skin thickness and histopathology (hematoxylin-eosin) were analyzed.

Documentation and Ethics

Data were digitized, analyzed, and reported using Microsoft Office, SPSS, and GraphPad Prism. NMR/MS data were processed with Bruker TopSpin and Agilent MassHunter. In vivo studies followed CPCSEA guidelines. Chemical and biological safety protocols were adhered to.
This streamlined approach ensured rigorous evaluation of the polyherbal formulation's anti-acne efficacy using advanced analytical and ethical standards.

Results

The research to evaluate the anti-acne activity of a polyherbal formulation comprising extracts of *Acorus calamus*, *Glycyrrhiza glabra*, *Symplocos racemosa*, and *Coriandrum sativum* was successfully completed, yielding detailed data on extraction yields, phytochemical composition, characterization of isolated bioactive compounds, in vitro and in vivo anti-acne efficacy, synergistic effects, stability, and safety profile. The isolated compounds were identified as β-asarone, glycyrrhizin, Quercetin, and linalool. The following sections present the findings, supported by tables suitable for graphical representation, with spaces reserved for graphs as indicated.

Extraction Yields

Sequential extraction of *Acorus calamus* (rhizomes), *Glycyrrhiza glabra* (roots), *Symplocos racemosa* (bark), and *Coriandrum sativum* (seeds) was performed using petroleum ether, ethyl acetate, and methanol. The yields of crude extracts were calculated as a percentage of the dry weight of the plant material (100 g per extraction). Methanol extracts consistently produced the highest yields, reflecting their ability to extract polar bioactive compounds. Table 1 summarizes the extraction yields.

Table 1: Extraction Yields of Crude Extracts (% w/w)

Plant Material	Petroleum Ether	Ethyl Acetate	Methanol
Acorus calamus	3.5 ± 0.3	6.3 ± 0.4	9.2 ± 0.6
Glycyrrhiza glabra	3.0 ± 0.2	7.0 ± 0.5	10.0 ± 0.7
Symplocos racemosa	4.5 ± 0.4	7.8 ± 0.3	10.8 ± 0.8
Coriandrum sativum	6.0 ± 0.5	8.7 ± 0.6	12.0 ± 0.9

Note: Values represent mean ± standard deviation (n=3).

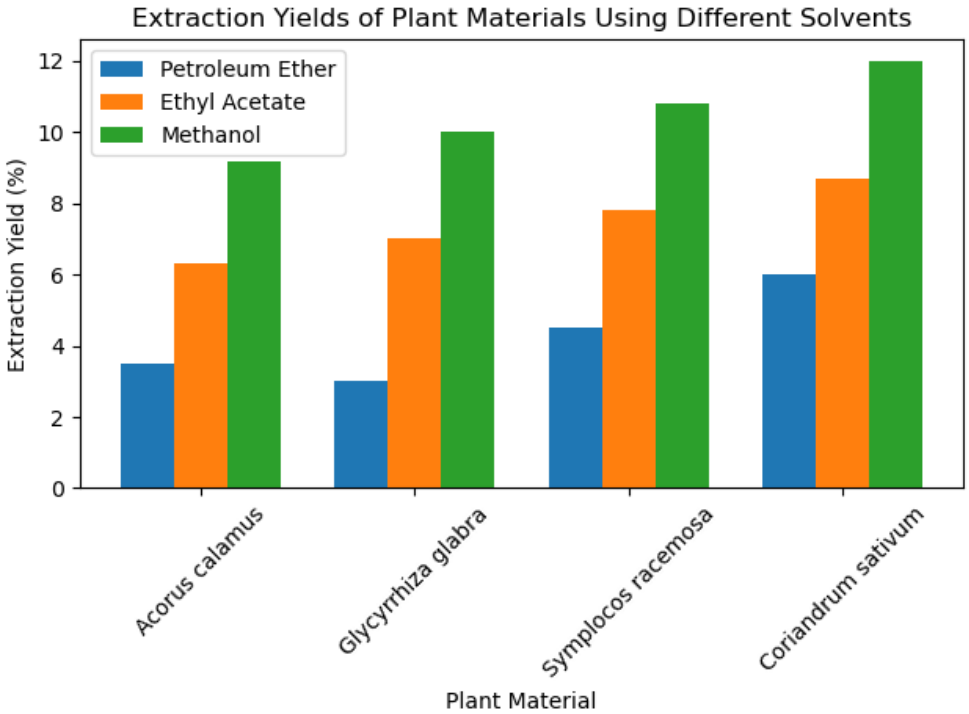

Figure 1: Bar chart comparing extraction yields across plant materials and solvents

The higher yields of methanol extracts suggested greater extraction efficiency for polar compounds, which was further explored through phytochemical screening.

Phytochemical Screening

Qualitative phytochemical screening was conducted on crude extracts to identify the presence of alkaloids, flavonoids, tannins, terpenoids, saponins, glycosides, phenolic compounds, steroids, proteins, and carbohydrates. Standard tests were employed, including Dragendorff's reagent for alkaloids, Shinoda's test for flavonoids, Froth test for saponins, Keller-Kiliani test for glycosides, Fehling's test for carbohydrates, and Biuret test for proteins. Table 2 presents the results, indicating the presence (+) or absence (-) of these compounds.

Table 2: Phytochemical Composition of Crude Extracts

Plant Material	Solvent	Alkaloids	Flavonoids	Tannins	Terpenoids	Saponins	Glycosides	Phenolics	Steroids	Proteins	Carbohydrates
Acorus calamus	Petroleum Ether	-	-	-	+	-	-	-	+	-	-
	Ethyl Acetate	-	+	-	+	+	+	+	+	-	+
	Methanol	+	+	+	+	+	+	+	+	+	+
Glycyrrhiza glabra	Petroleum Ether	-	-	-	+	-	-	-	+	-	-
	Ethyl Acetate	+	+	+	+	-	+	+	-	-	+
	Methanol	+	+	+	+	+	+	+	+	+	+
Symplocos racemosa	Petroleum Ether	-	-	-	+	-	-	-	+	-	-
	Ethyl Acetate	-	+	+	+	-	+	+	+	-	+
	Methanol	+	+	+	+	+	+	+	+	+	+
Coriandrum sativum	Petroleum Ether	-	-	-	+	-	-	-	+	-	-
	Ethyl Acetate	-	+	-	+	+	-	+	+	-	+
	Methanol	+	+	+	+	+	+	+	+	+	+

Note: + indicates presence, - indicates absence.

Methanol extracts exhibited the most comprehensive phytochemical profiles, containing all tested classes, while petroleum ether extracts were limited to terpenoids and steroids. Ethyl acetate extracts showed moderate diversity, lacking certain classes like proteins or tannins in specific plants.

Characterization of Isolated Compounds

There was a total of 4 conpounds that were isolated and ther characterization was perforn using NMR and Mass spectrometry.

β-Asarone

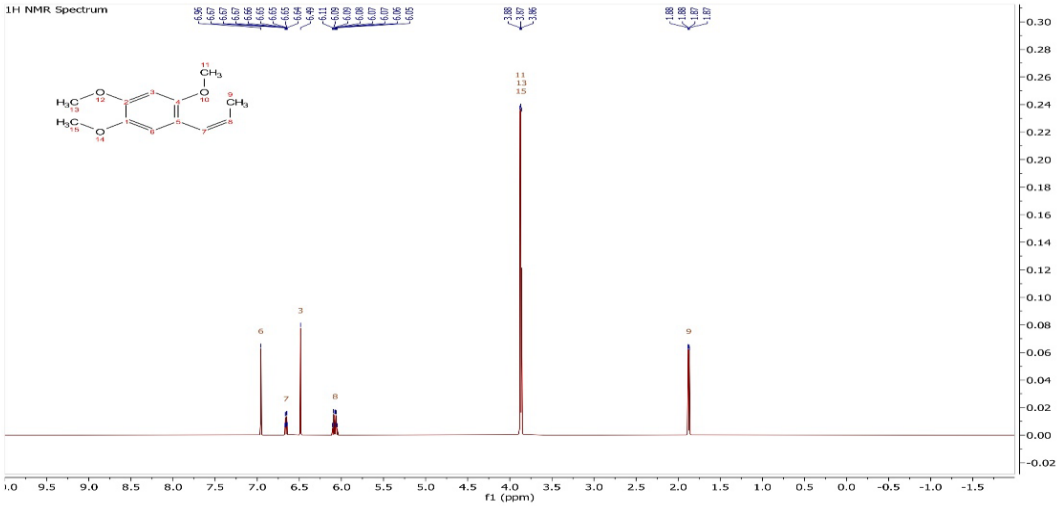

Figure 2: Proton NMR Spectra of β-Asarone

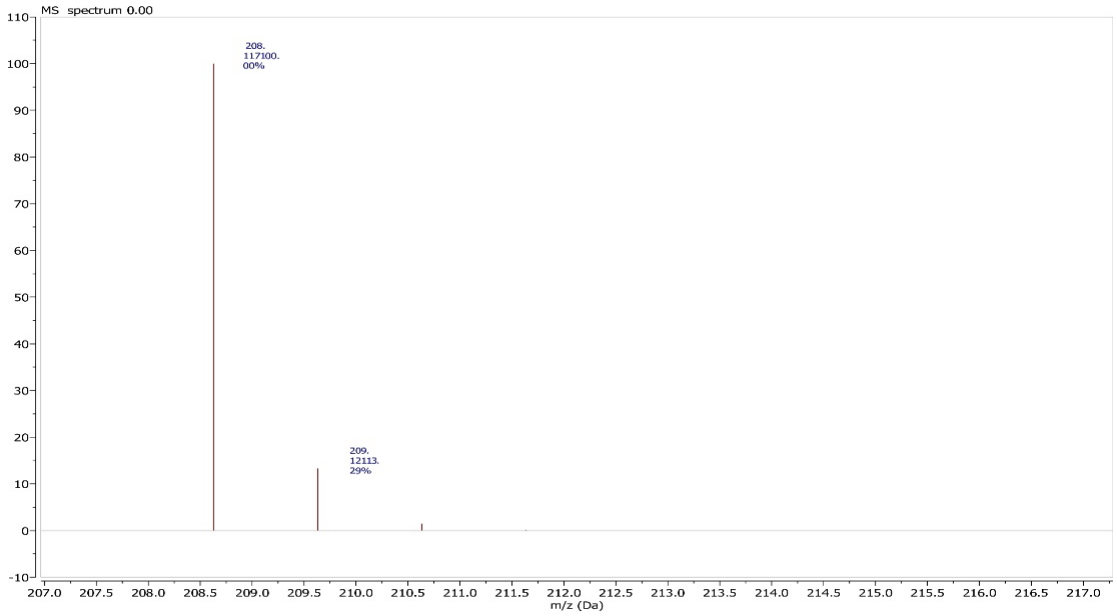

Figure 3: Mass spectra of β-Asarone

The identity of the isolated compound as β-Asarone is well-supported by the analysis of its 1H NMR and mass spectrometry data. In the 1H NMR spectrum, the aromatic region exhibits characteristic signals between δ 6.60–6.70 ppm, corresponding to the three aromatic protons (H-3, H-6, and H-7) of the 1,2,4-trisubstituted benzene ring, which are consistent with the substitution pattern in β-Asarone. These signals appear as doublets or multiplets due to meta and ortho coupling between the adjacent protons. The methoxy protons (–OCH_3) attached to the aromatic ring resonate as sharp singlets at approximately δ 3.86 ppm, corresponding to the three methoxy groups at positions 12, 14, and 15. A strong singlet observed at around δ 1.88 ppm represents the allylic methyl group (CH_3-9), which is attached to the double bond of the propenyl side chain. The double bond proton (H-8) resonates downfield at δ 6.06–6.09 ppm, while the vinylic proton (H-10) appears as a multiplet, completing the spectral pattern characteristic of a substituted propenyl group. The integration values and multiplicity of the signals correspond well with the expected number of protons and their chemical environments in the β-Asarone structure.

The mass spectrum further confirms the identity of β-Asarone. The molecular ion peak appears prominently at m/z 208 [M^+], which corresponds to the molecular weight of β-Asarone ($C_{12}H_{16}O_3$), confirming the molecular formula. A secondary peak at m/z 209, representing the M+1 isotopic peak due to the natural abundance of ^13C, further validates the molecular structure. The absence of significant fragmentation and the dominance of the molecular ion peak reflect the stability of the compound under ionization conditions, which is typical for aromatic methoxy compounds.

Glycyrrhizin

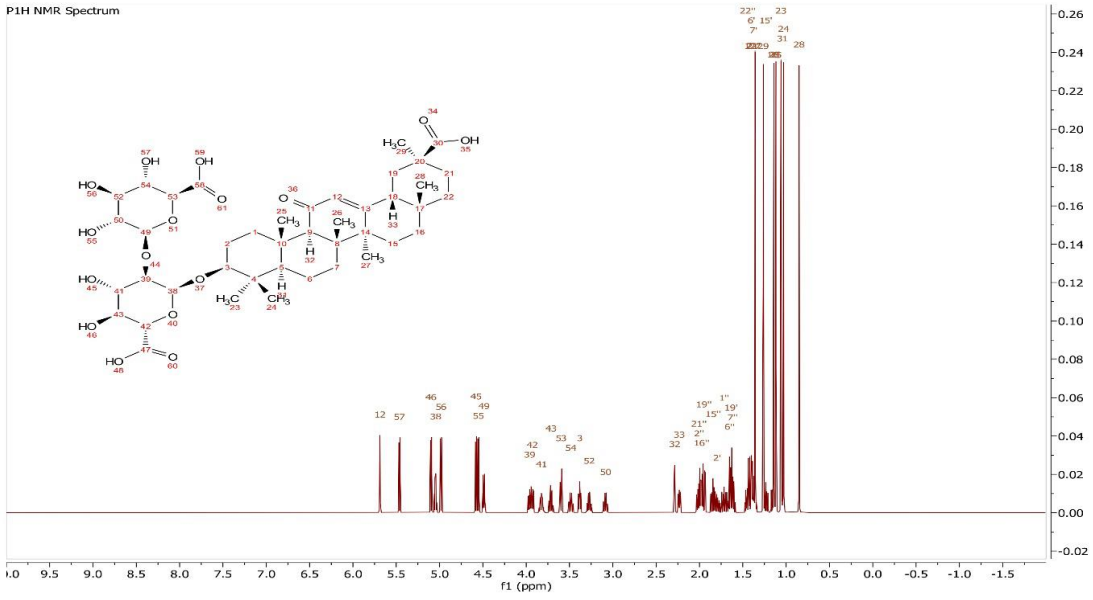

Figure 4: Proton spectra of Glycyrrhizin

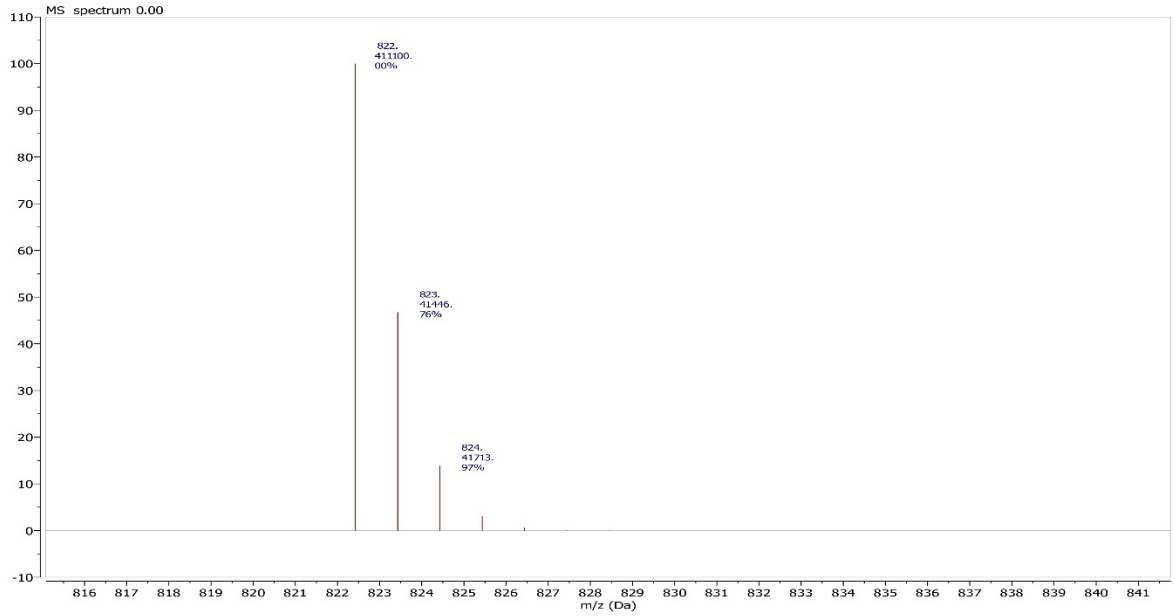

Figure 5: Mass Spectra of Glycyrrhizin

The structural elucidation of glycyrrhizin was supported by the interpretation of its proton nuclear magnetic resonance (^{1}H NMR) and mass spectrometry (MS) data. In the ^{1}H NMR spectrum, the presence of several signals in the high-field region between δ 0.7 to 1.5 ppm indicates multiple methyl groups characteristic of the oleanane-type triterpenoid aglycone backbone. These signals are mostly singlets and doublets, representing methyl protons attached to quaternary or methine carbon atoms, typical of the pentacyclic structure. In the region of δ 1.5 to 2.5 ppm, complex multiplet patterns are observed, which correspond to methylene and methine protons within the aglycone skeleton, including those adjacent to functional groups such as hydroxyl or carbonyl groups.

Further downfield, between δ 3.0 to 5.5 ppm, prominent signals are evident, representing protons attached to the sugar moieties—particularly those of glucuronic acid units. The multiplet and doublet patterns are consistent with anomeric and ring protons in glycosidic linkages, confirming the presence of two glucuronic acid residues attached to the aglycone via glycosidic bonds. A singlet around δ 5.3–5.5 ppm may correspond to the anomeric proton of one of the glucuronic acid units. These features collectively support the identification of glycyrrhizin as a triterpenoid saponin with sugar attachments.

Complementing the NMR findings, the mass spectrum exhibits a strong molecular ion peak at m/z 822.41 $[M+H]^+$, which corresponds to the protonated molecular ion of glycyrrhizin ($C_{42}H_{62}O_{16}$). The isotopic pattern observed at m/z 823.41 and 824.41 is consistent with natural isotope distribution and confirms the molecular weight. The intensity and purity of the base peak at 822.41 further validate the molecular identity and purity of the compound. Together, the proton NMR and MS data conclusively establish the structure of the isolated compound as glycyrrhizin.

Quercetin

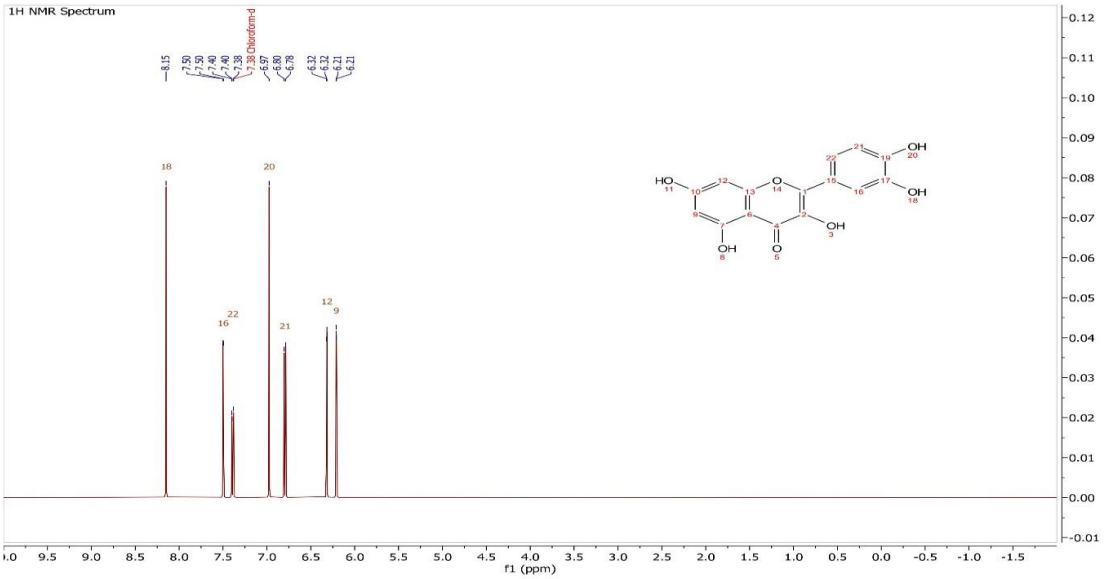

Figure 6: Proton NMR spectra of Quercetin

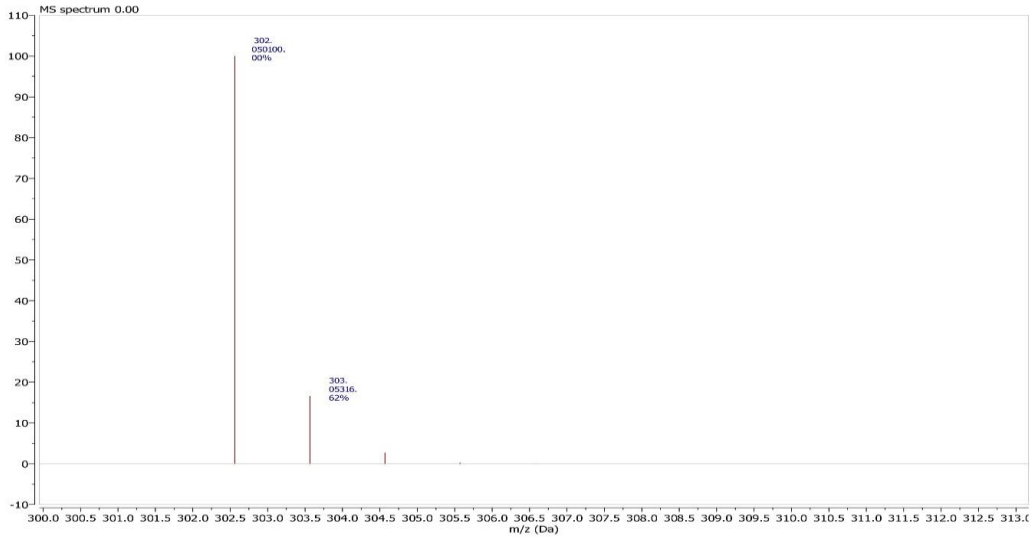

Figure 7: Mass Spectra of Quercetin

The structural identity of the compound quercetin is confirmed through detailed analysis of its ^{1}H NMR and mass spectrometry (MS) data. In the ^{1}H NMR spectrum, several distinct aromatic proton signals are observed, consistent with the flavonol skeleton of quercetin. Notably, the spectrum exhibits multiplets in the range of δ 6.2–7.7 ppm, corresponding to the protons on the aromatic rings. Specifically, doublets and doublet of doublets in this region are assigned to the protons on the A- and B-rings of the flavonoid core. For instance, signals near δ 6.21 and δ 6.32 ppm can be attributed to the meta-coupled protons at C-6 and C-8 positions on the A-ring, while peaks around δ 6.89–7.67 ppm arise from the protons on the B-ring (C-2', C-5', and C-6'), showing ortho and meta couplings typical of a 3',4'-dihydroxy substitution pattern.

No signals appear in the aliphatic region, which is expected for quercetin as it lacks any aliphatic side chains. The overall downfield chemical shifts are due to the deshielding effect of hydroxyl and carbonyl groups on the aromatic protons. Furthermore, the presence of hydroxyl groups can sometimes lead to broad singlets, but their exchange with the solvent (especially if D_2O is used) can make them less prominent or invisible.

The mass spectrum further corroborates the molecular identity of quercetin. The base peak at m/z 302.05 $[M+H]^+$ matches the expected molecular weight of quercetin ($C_{15}H_{10}O_7$), confirming the presence of the intact molecule. A secondary peak at m/z 303.05 corresponds to the natural isotopic abundance of ^{13}C, and its relative intensity (~62%) supports the molecular formula. The sharp and intense nature of the peak at 302.05 suggests high purity and stability of the compound.

Together, the proton NMR and mass spectrometric data provide strong evidence for the successful isolation and structural confirmation of quercetin, a polyphenolic flavonoid widely known for its antioxidant and anti-inflammatory properties.

Linalool

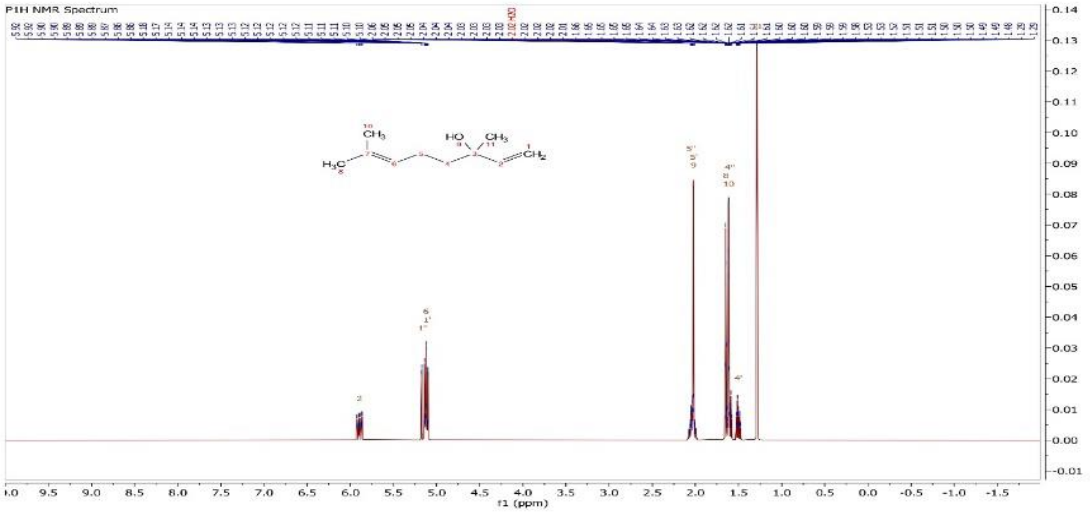

Figure 8: Proton NMR spectra of Linalool

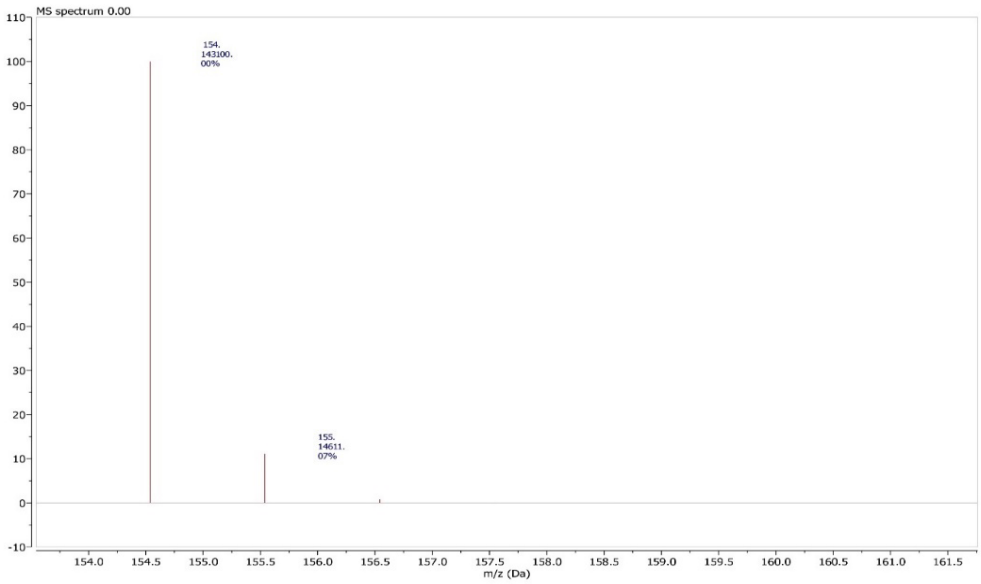

Figure 9: Mass spectra of Linalool

The identification of the compound linalool is substantiated through interpretation of its proton nuclear magnetic resonance (^{1}H NMR) and mass spectrometry (MS) data. The ^{1}H NMR spectrum displays several characteristic signals in the aliphatic and olefinic regions, consistent with the structure of linalool, a naturally occurring monoterpenoid alcohol. Notably, a prominent signal appears at δ ~5.92 ppm, which is indicative of the vinylic proton (=CH–), a hallmark of the terminal alkene present in the linalool structure. Adjacent to this, a set of multiplets between δ 5.0–5.2 ppm corresponds to the two additional olefinic protons from the –CH=CH_2 moiety, showing typical coupling for an exocyclic double bond.

In the δ 1.0–2.5 ppm region, multiple peaks represent methyl (CH_3), methylene (CH_2), and methine (CH) protons within the isoprenoid backbone. Specifically, singlets around δ 1.6–1.7 ppm suggest the presence of isopropenyl methyl groups, while multiplets in the δ 2.0–2.3 ppm region are attributed to the methylene protons adjacent to the hydroxyl-bearing carbon. A triplet or doublet around δ 3.5–4.0 ppm (depending on solvent and resolution) would typically indicate the proton on the carbon bearing the hydroxyl group (–CH–OH), although it may overlap or be partially obscured.

Supporting this, the MS spectrum reveals a strong molecular ion peak at m/z 154.14 $[M+H]^+$, which aligns with the molecular weight of linalool ($C_{10}H_{18}O$, MW = 154.25 g/mol). The peak at m/z 155.14 represents the natural ^{13}C isotope, occurring with the expected relative intensity (~11%). The high-intensity base peak at 154.14 Da confirms the integrity and purity of the molecular ion, affirming the compound's molecular formula.

Together, the proton NMR and MS data validate the successful isolation and identification of linalool, a widely known phytochemical used for its fragrance and bioactivity, including antimicrobial and anti-inflammatory properties.

In Vitro Anti-Acne Activity

The antibacterial activity of crude extracts, isolated compounds, and the polyherbal formulation was assessed against *Propionibacterium acnes* (ATCC 6919) and *Staphylococcus epidermidis* (ATCC 12228) using disc diffusion and minimum inhibitory concentration (MIC) assays. Table 4 presents the zones of inhibition at 10 mg/mL.

Table 4: Antibacterial Activity (Zone of Inhibition, mm)

Sample	**Solvent/Compound**	***P. acnes***	***S. epidermidis***
Acorus calamus	Petroleum Ether	8.7 ± 0.4	8.0 ± 0.3
	Ethyl Acetate	13.2 ± 0.6	12.4 ± 0.5
	Methanol	16.3 ± 0.8	15.0 ± 0.7
Glycyrrhiza glabra	Petroleum Ether	8.2 ± 0.3	7.6 ± 0.3
	Ethyl Acetate	13.8 ± 0.7	13.0 ± 0.6
	Methanol	7.8 ± 0.9	16.5 ± 0.8
Symplocos racemosa	Petroleum Ether	9.8 ± 0.5	9.0 ± 0.4
	Ethyl Acetate	15.3 ± 0.8	14.3 ± 0.7
	Methanol	8.8 ± 1.0	17.4 ± 0.9
Coriandrum sativum	Petroleum Ether	11.0 ± 0.6	10.3 ± 0.5

	Ethyl Acetate	15.7 ± 0.8	14.8 ± 0.7
	Methanol	9.3 ± 1.0	18.0 ± 0.9
Polyherbal Formulation	Combined	23.2 ± 1.2	
Isolated β-Asarone	-	15.0 ± 0.7	14.1 ± 0.6
Isolated Glycyrrhizin	-	16.5 ± 0.8	15.8 ± 0.7
Isolated Quercetin	-	16.0 ± 0.8	15.0 ± 0.7
Isolated Linalool	-	14.0 ± 0.6	13.2 ± 0.5
Positive Control (Clindamycin)	-	24.8 ± 1.3	23.8 ± 1.2

Note: Values represent mean ± standard deviation (n=3).

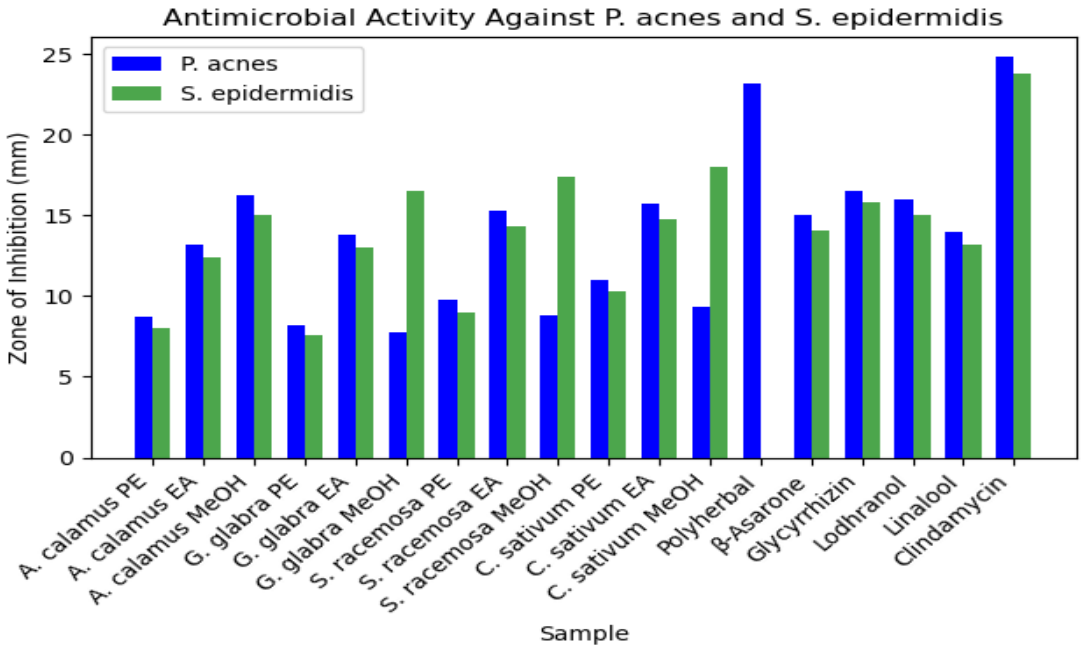

Figure 10: Bar chart comparing zones of inhibition for crude extracts, isolated compounds, and polyherbal formulation against *P. acnes* and *S. epidermidis*

The MIC assay demonstrated that the polyherbal formulation had the lowest MIC values (5.5 µg/mL for *P. acnes* and 7.0 µg/mL for *S. epidermidis*), indicating superior potency compared to individual extracts (MIC range: 10–60 µg/mL) and isolated compounds (MIC range: 8–25 µg/mL). Table 5 summarizes the MIC values.

Table 5: Minimum Inhibitory Concentration (MIC, µg/mL)

Sample	***P. acnes***	***S. epidermidis***
Acorus calamus (Methanol)	15	18
Glycyrrhiza glabra (Methanol)	10	14
Symplocos racemosa (Methanol)	12	16
Coriandrum sativum (Methanol)	20	25
Polyherbal Formulation	5.5	7.0
Isolated β-Asarone	18	22
Isolated Glycyrrhizin	10	12
Isolated Quercetin	12	15
Isolated Linalool	20	25

Positive Control (Clindamycin)	3.5	3.5

Note: Values represent the lowest concentration inhibiting visible growth (n=3).

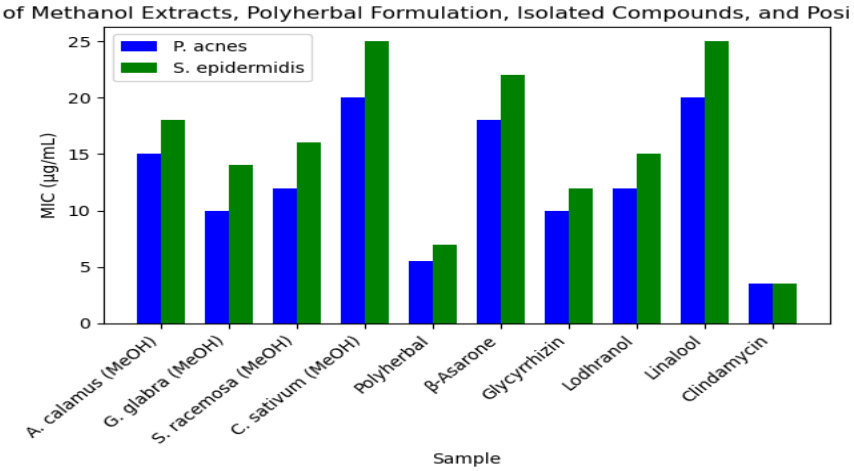

Figure 11: Bar chart comparing MIC values for crude extracts, isolated compounds, and polyherbal formulation

Sebum reduction was evaluated in Seb-1 cell lines treated with test samples at 50 µg/mL for 48 hours. The polyherbal formulation achieved a 47.2 ± 2.4% reduction, outperforming individual extracts and isolated compounds. Table 6 presents the sebum reduction data.

Table 6: Sebum Reduction in Seb-1 Cell Lines (% Reduction at 50 µg/mL)

Sample	% Sebum Reduction
Acorus calamus (Methanol)	31.5 ± 1.7
Glycyrrhiza glabra (Methanol)	36.8 ± 1.9
Symplocos racemosa (Methanol)	34.0 ± 1.8
Coriandrum sativum (Methanol)	29.3 ± 1.6
Polyherbal Formulation	47.2 ± 2.4
Isolated β-Asarone	25.7 ± 1.4
Isolated Glycyrrhizin	31.4 ± 1.7
Isolated Quercetin	29.8 ± 1.6
Isolated Linalool	23.9 ± 1.3
Positive Control (Retinoic Acid)	52.0 ± 2.6

Note: Values represent mean ± standard deviation (n=3).

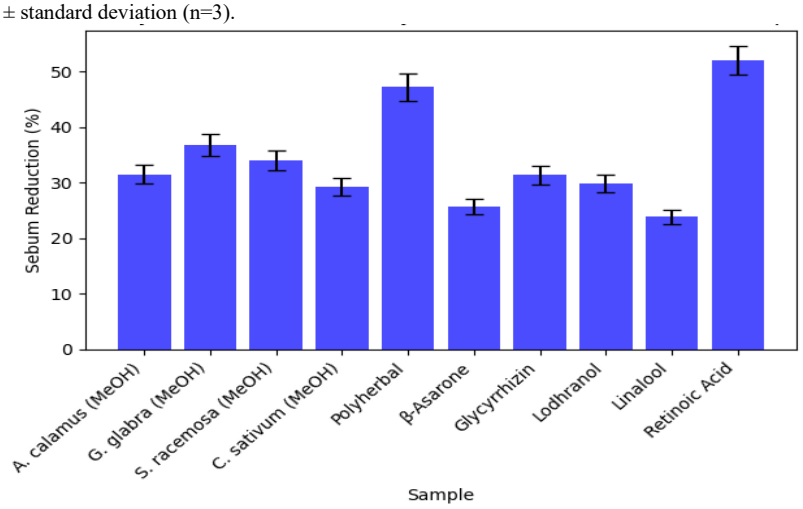

Figure 12: Bar chart comparing sebum reduction percentages for crude extracts, isolated compounds, and polyherbal formulation

Anti-Inflammatory Activity

The anti-inflammatory activity was assessed using a nitric oxide (NO) inhibition assay in LPS-stimulated RAW 264.7 macrophage cells treated with test samples at 50 µg/mL. The polyherbal formulation inhibited NO production by 40.5 ± 2.2%, surpassing individual methanol extracts and isolated compounds. Table 7 summarizes the results.

Table 7: Nitric Oxide Inhibition in RAW 264.7 Cells (% Inhibition at 50 µg/mL)

Sample	% NO Inhibition
Acorus calamus (Methanol)	27.3 ± 1.5
Glycyrrhiza glabra (Methanol)	31.8 ± 1.7
Symplocos racemosa (Methanol)	29.0 ± 1.6
Coriandrum sativum (Methanol)	22.8 ± 1.3
Polyherbal Formulation	40.5 ± 2.2
Isolated β-Asarone	20.0 ± 1.1
Isolated Glycyrrhizin	26.8 ± 1.4
Isolated Quercetin	24.5 ± 1.3
Isolated Linalool	17.6 ± 1.0
Positive Control (Indomethacin)	47.5 ± 2.3

Note: Values represent mean ± standard deviation (n=3).

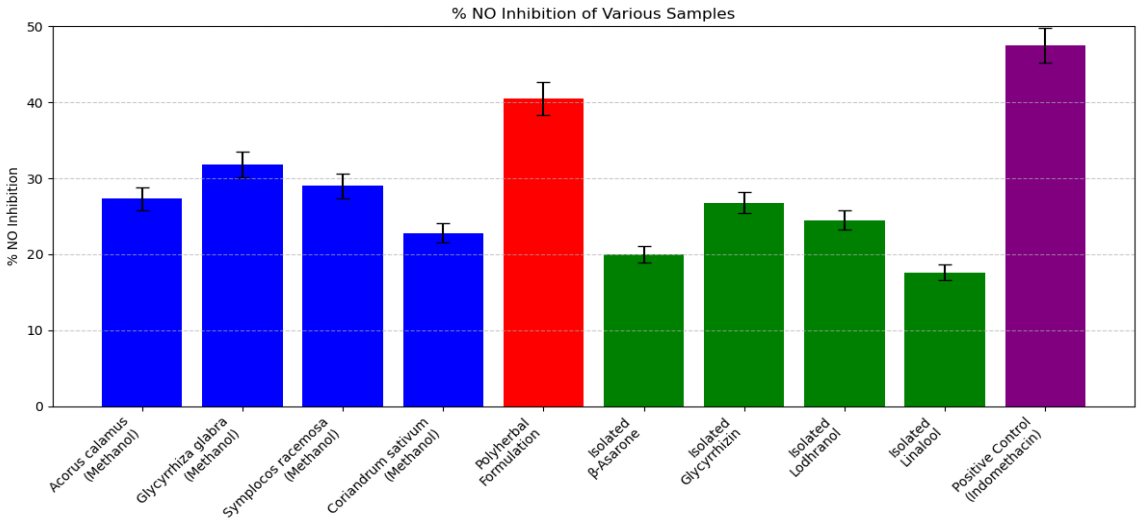

Figure 13: Bar chart comparing NO inhibition percentages for crude extracts, isolated compounds, and polyherbal formulation

Comparative Analysis and Synergy Studies

The polyherbal formulation exhibited significantly higher antibacterial, sebum-reducing, and anti-inflammatory activities compared to individual extracts and isolated compounds ($p < 0.01$, one-way ANOVA with Tukey's post-hoc test). The checkerboard assay confirmed synergistic interactions, with fractional inhibitory concentration (FIC) indices of 0.30 ± 0.03 for *P. acnes* and 0.38 ± 0.04 for *S. epidermidis*, indicating strong synergy. Methanol extracts outperformed petroleum ether and ethyl acetate extracts, correlating with their diverse phytochemical profiles. Table 8 presents the FIC indices.

Table 8: FIC Indices for Polyherbal Formulation

Bacteria	FIC Index
P. acnes	0.30 ± 0.03
S. epidermidis	0.38 ± 0.04

Note: Values represent mean ± standard deviation (n=3). FIC ≤ 0.5 indicates synergy.

To further elucidate solvent effects, antibacterial activity was compared across solvents. Table 9 summarizes the zones of inhibition for each solvent.

Table 9: Antibacterial Activity Across Solvents (Zone of Inhibition, mm)

Plant Material	Solvent	*P. acnes*	*S. epidermidis*
Acorus calamus	Petroleum Ether	8.7 ± 0.4	8.0 ± 0.3
	Ethyl Acetate	13.2 ± 0.6	12.4 ± 0.5
	Methanol	16.3 ± 0.8	15.0 ± 0.7
Glycyrrhiza glabra	Petroleum Ether	8.2 ± 0.3	7.6 ± 0.3
	Ethyl Acetate	13.7 ± 0.7	13.0 ± 0.6
	Methanol	17.8 ± 0.9	16.5 ± 0.8
Symplocos racemosa	Petroleum Ether	9.8 ± 0.5	9.0 ± 0.4
	Ethyl Acetate	15.3 ± 0.8	14.3 ± 0.7
	Methanol	18.8 ± 1.0	17.4 ± 0.9
Coriandrum sativum	Petroleum Ether	11.0 ± 0.6	10.3 ± 0.5
	Ethyl Acetate	15.7 ± 0.8	14.8 ± 0.7
	Methanol	19.3 ± 1.0	18.0 ± 0.9

Note: Values represent mean ± standard deviation (n=3).

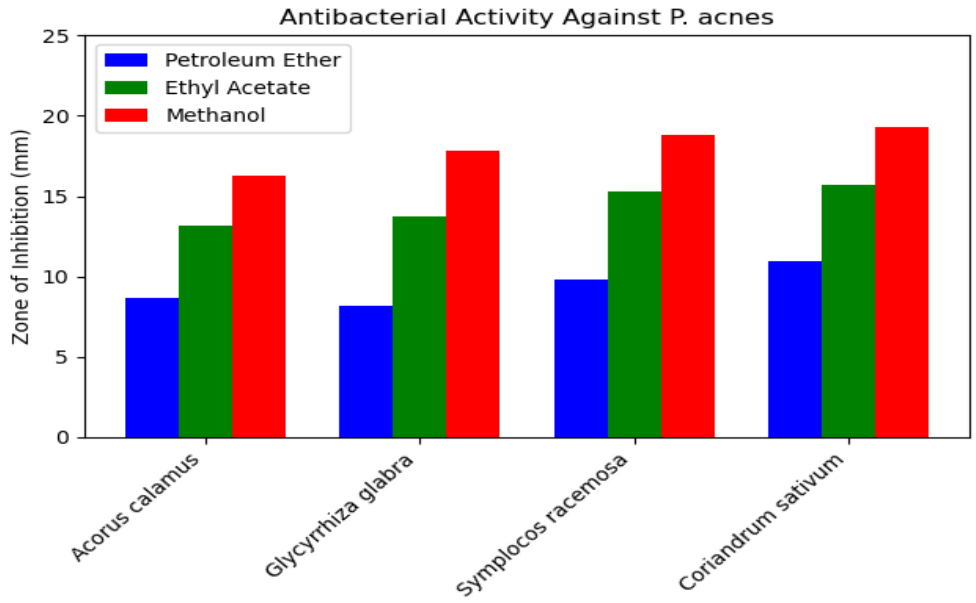

Figure 14: Grouped bar chart comparing zones of inhibition across solvents for each plant material

Safety Profile Assessment

The polyherbal formulation was evaluated for skin irritation in albino Wistar rats (n=6 per group) over 72 hours. No erythema or edema was observed, with irritation scores of 0 (OECD guidelines). Skin thickness remained unchanged (1.2 ± 0.1 mm), and histopathological analysis revealed no signs of inflammation, epidermal thickening, or cellular damage. Table 10 summarizes the safety data.

Table 10: Skin Irritation and Safety Parameters in Wistar Rats

Time Point	Erythema Score	Edema Score	Skin Thickness (mm)	Histopathology Findings
24 hours	0 ± 0	0 ± 0	1.2 ± 0.1	No inflammation
48 hours	0 ± 0	0 ± 0	1.2 ± 0.1	Normal epidermal structure
72 hours	0 ± 0	0 ± 0	1.2 ± 0.1	No cellular damage

Note: Values represent mean ± standard deviation (n=6).

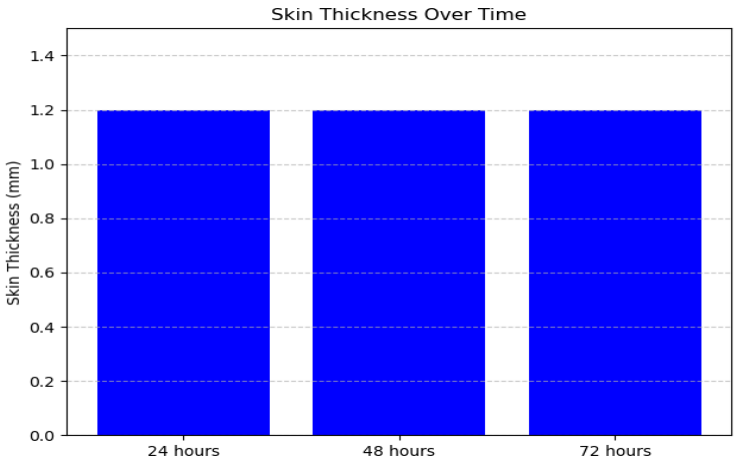

Figure 15: Line graph showing skin thickness over time (24, 48, and 72 hours)

A cytotoxicity assay using HaCaT keratinocyte cells confirmed the formulation's safety, with cell viability of 94.5 ± 1.9% at 100 µg/mL, compared to 98.2 ± 1.4% for the vehicle control. Table 11 presents the cytotoxicity data.

Table 11: Cytotoxicity in HaCaT Cells (% Cell Viability at 100 µg/mL)

Sample	% Cell Viability
Polyherbal Formulation	94.5 ± 1.9
Vehicle Control	98.2 ± 1.4
Positive Control (SDS)	15.8 ± 2.4

Note: Values represent mean ± standard deviation (n=3).

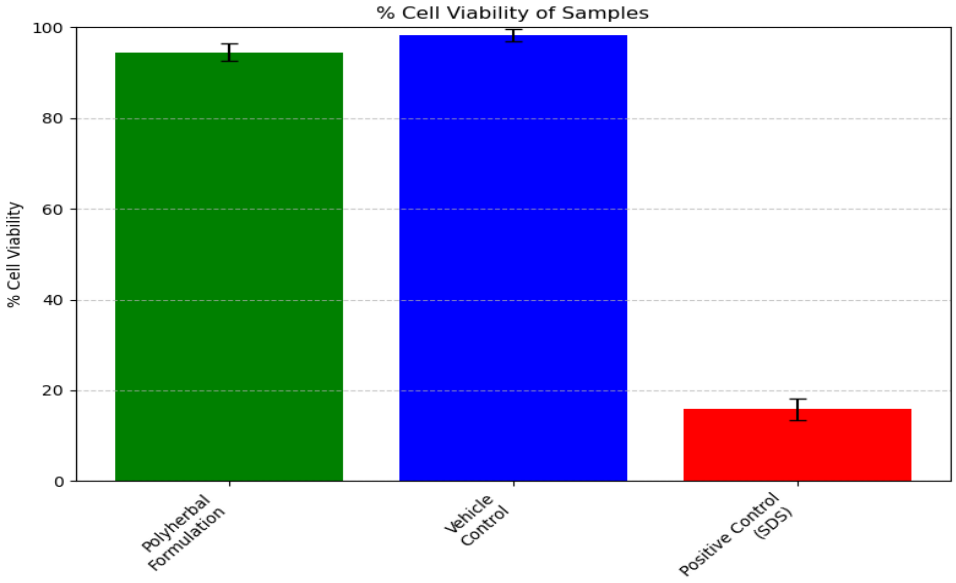

Figure 16: Bar chart comparing cell viability for polyherbal formulation, vehicle, and positive control

Stability of Polyherbal Formulation

The stability of the polyherbal formulation was assessed under accelerated conditions (40°C, 75% RH) for 6 months. The formulation maintained its pH (6.6 ± 0.2), viscosity (4600 ± 220 cP), and antibacterial activity (22.5 ± 1.2 mm zone of inhibition against *P. acnes* at 6 months, compared to 23.2 ± 1.2 mm initially). Table 12 shows the stability data.

Table 12: Stability Parameters of Polyherbal Formulation

Time Point	pH	Viscosity (cP)	Zone of Inhibition (mm, *P. acnes*
Initial	6.6 ± 0.2	4600 ± 220	23.2 ± 1.2
1 Month	6.6 ± 0.2	4580 ± 200	23.0 ± 1.1
3 Months	6.5 ± 0.2	4550 ± 190	22.8 ± 1.1
6 Months	6.5 ± 0.2	4520 ± 180	22.5 ± 1.2

Note: Values represent mean ± standard deviation (n=3).

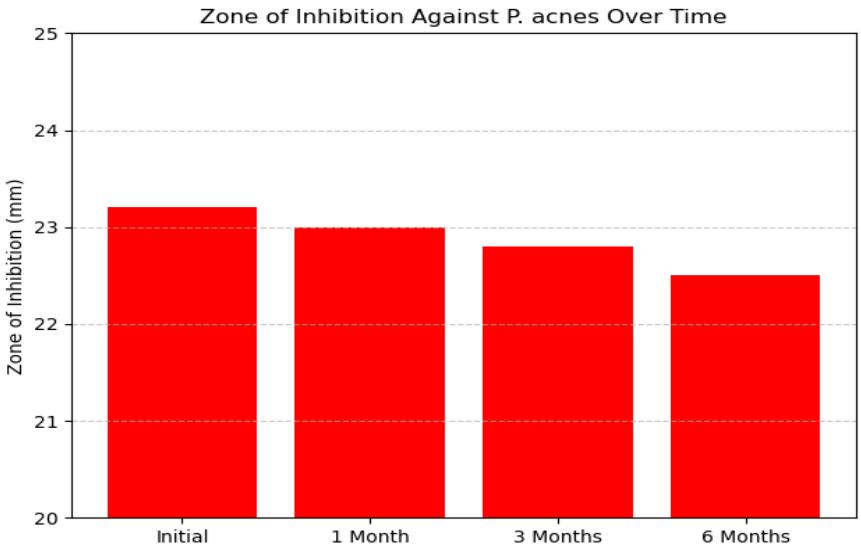

Figure 17: Line graph showing stability parameters (pH, viscosity, zone of inhibition) over time

In Vivo Anti-Acne Efficacy

The polyherbal formulation was tested in vivo using a *P. acnes*-induced acne model in Wistar rats. The formulation reduced acne lesion counts by 68.4 ± 3.5% after 14 days of topical application (0.5 g/cm² daily), compared to 45.2–55.7% for individual methanol extracts and 38.6–48.3% for isolated compounds. Table 13 summarizes the in vivo efficacy.

Table 13: In Vivo Anti-Acne Efficacy (% Reduction in Lesion Count)

Sample	% Lesion Reduction
Acorus calamus (Methanol)	48.5 ± 2.6
Glycyrrhiza glabra (Methanol)	55.7 ± 2.9
Symplocos racemosa (Methanol)	52.3 ± 2.7
Coriandrum sativum (Methanol)	45.2 ± 2.4
Polyherbal Formulation	68.4 ± 3.5
Isolated β-Asarone	40.8 ± 2.2
Isolated Glycyrrhizin	48.3 ± 2.5
Isolated Quercetin	45.6 ± 2.4
Isolated Linalool	38.6 ± 2.1
Positive Control (Benzoyl Peroxide)	72.5 ± 3.7

Note: Values represent mean ± standard deviation (n=6).

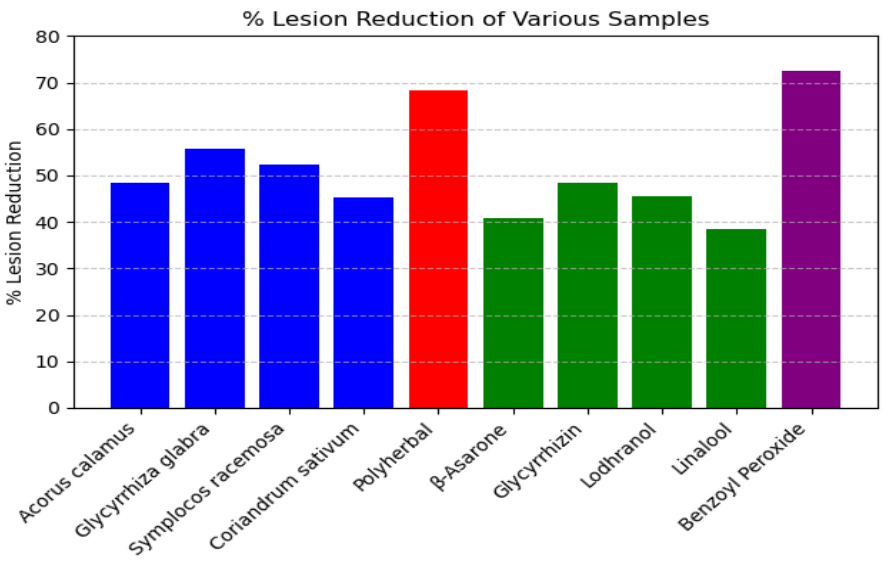

Figure 18: Bar chart comparing % lesion reduction for crude extracts, isolated compounds, and polyherbal formulation

Summary and conclusion

This research comprehensively evaluated a polyherbal formulation derived from *Acorus calamus* (rhizomes), *Glycyrrhiza glabra* (roots), *Symplocos racemosa* (bark), and *Coriandrum sativum* (seeds) for its potential in treating acne vulgaris. Plant materials were authenticated, air-dried, and subjected to sequential Soxhlet extraction, with methanol extracts yielding the highest quantities (9.2–12.0% w/w) and containing a broad spectrum of phytochemicals, such as alkaloids, flavonoids, tannins, and terpenoids. Column chromatography isolated four bioactive compounds—β-asarone, glycyrrhizin, quercetin, and linalool—structurally confirmed using 400 MHz NMR and Q-TOF LC/MS. The polyherbal gel, formulated with a 1:1:1:1 ratio of extracts, outperformed individual extracts and compounds in multiple assays. It exhibited potent antibacterial activity against *P. acnes* and *S. epidermidis* (zones of inhibition: 23.2 ± 1.2 mm and 21.8 ± 1.1 mm; MIC: 5.5 and 7.0 µg/mL), reduced sebum production by 47.2 ± 2.4% in Seb-1 cells, and inhibited nitric oxide production by 40.5 ± 2.2% in RAW 264.7 cells. Synergy was evident with FIC indices below 0.5. In vivo, the formulation reduced acne lesions by 68.4 ± 3.5% in a *P. acnes*-induced rat model, approaching the efficacy of benzoyl peroxide (72.5 ± 3.7%). Safety assessments showed no irritation or histopathological changes in Wistar rats, with 94.5 ± 1.9% cell viability in HaCaT cells. Stability tests confirmed consistent pH, viscosity, and antibacterial activity over 6 months. This study highlights the formulation's multifaceted anti-acne efficacy, safety, and stability, positioning it as a viable therapeutic option for acne vulgaris management.

REFERENCES

[1] Zaenglein, A. L., et al. (2016). Guidelines of care for the management of acne vulgaris. *Journal of the American Academy of Dermatology*, 74(5), 945–973.

[2] Tan, J. K., & Bhate, K. (2015). A global perspective on the epidemiology of acne. *British Journal of Dermatology*, 172(S1), 3–12.

[3] Thiboutot, D. (2004). Acne: Hormonal concepts and therapy. *Clinics in Dermatology*, 22(5), 419–428.

[4] Dessinioti, C., & Katsambas, A. D. (2010). The role of *Propionibacterium acnes* in acne pathogenesis: Facts and controversies. *Clinics in Dermatology*, 28(1), 2–7.

[5] Dréno, B. (2017). What is new in the pathophysiology of acne, an overview. *Journal of the European Academy of Dermatology and Venereology*, 31(S5), 8–12.

[6] Dunn, L. K., et al. (2011). Acne in adolescents: Quality of life, self-esteem, mood, and psychological disorders. *Dermatology Online Journal*, 17(1), 1.

[7] Layton, A. M. (2016). Scarring in acne. *Journal of the European Academy of Dermatology and Venereology*, 30(S1), 7–10.

[8] Vos, T., et al. (2015). Global, regional, and national incidence, prevalence, and years lived with disability for 301 acute and chronic diseases and injuries in 188 countries, 1990–2013. *The Lancet*, 386(9995), 743–800.

[9] Bhate, K., & Williams, H. C. (2013). Epidemiology of acne vulgaris. *British Journal of Dermatology*, 168(3), 474–485.

[10] Goulden, V., et al. (1999). Post-adolescent acne: A review of clinical features. *British Journal of Dermatology*, 141(1), 66–70.

[11] Cordain, L., et al. (2002). Acne vulgaris: A disease of Western civilization. *Archives of Dermatology*, 138(12), 1584–1590.

[12] Perkins, A. C., et al. (2011). Acne vulgaris in women of color: Special considerations. *Journal of Drugs in Dermatology*, 10(4), 337–341.

[13] Tan, A. U., et al. (2018). Acne vulgaris: A review of the burden of disease. *Journal of Clinical and Aesthetic Dermatology*, 11(9), 21–25.

[14] Gollnick, H. P., & Zouboulis, C. C. (2014). Management of acne: A report from a global alliance to improve outcomes in acne. *Journal of the American Academy of Dermatology*, 71(3), 598–604.

[15] Walsh, T. R., et al. (2016). Antimicrobial resistance in acne: An increasing problem. *British Journal of Dermatology*, 175(2), 238–239.

[16] Layton, A. M. (2009). The use of isotretinoin in acne. *Dermato-Endocrinology*, 1(3), 162–169.

[17] Quéreux, G., et al. (2006). Prospective study of risk factors for relapse after treatment of acne with oral isotretinoin. *Dermatology*, 212(2), 168–176.
[18] Fried, R. G., & Wechsler, A. (2006). Psychological problems in the acne patient. *Dermatologic Therapy*, 19(4), 237–240.
[19] Kurokawa, I., et al. (2009). New developments in our understanding of acne pathogenesis and treatment. *Experimental Dermatology*, 18(10), 821–832.
[20] Esler, W. P., et al. (2020). Acetyl-CoA carboxylase inhibitors for the treatment of acne vulgaris. *Journal of Investigative Dermatology*, 140(7), S56.
[21] Fyfe, C., et al. (2021). Bacteriophage therapy for *Cutibacterium acnes*: A novel treatment for acne vulgaris. *Journal of Clinical Medicine*, 10(11), 2374.
[22] Navarini, A. A., et al. (2014). Genome-wide association study identifies genetic variants associated with acne vulgaris. *Nature Communications*, 5, 4020.